JOURNAL OF MATERIALS SCIENCE 26 (1991) 4383–4388

Morphology of polyamide 6-polybutadiene multiblock copolymers

K. A. H. LINDBERG
Swedish Institute for Wood Technology Research, Skeria 2, S-931 87 Skellefteå, Sweden
H. E. BERTILSSON*
Department of Polymeric Materials, Chalmers University of Technology, S-412 96 Gothenburg, Sweden

The morphology of polyamide 6-polybutadiene multiblock copolymers, commonly used for reaction injection moulding, have been investigated using transmission electron microscopy, dynamic mechanical techniques, calorimetry and wide angle X-ray diffraction. Phase separation is found to be almost complete and the crystallization of the PA6 blocks is slightly higher than in pure PA6. The morphology shows similarities to what has been reported for segmented polyether-esters. The PA6 lamellar dimensions found in the micrographs agree with dimensions calculated from melting point depression and X-ray data.

1. Introduction

The favourable mechanical properties of many multiblock copolymers are explained by microphase separation and the presence of domains. Typical polymers of this kind are segmented polyurethanes, polyether-esters and polyamides with polyether segments. With low strain elastic moduli in the range of 50–1000 MPa and highly elastic properties they have found significant technical importance as thermoplastics. The segmented polyurethanes and segmented polyamides have also been used as reaction injection moulding (RIM) materials. The good elastic properties are due to the alternating hard and soft segments of the polymer chains. The soft segments are typically low glass transition polymers, i.e. polyethers. The hard segments may possess a high glass transition temperature or be able to form crystalline domains. Control of the length of the segments and ratio between hard and soft segments enables the production of materials with highly variable mechanical properties. Regardless of the composition and length of segment, the microdomain morphology, the character of the phase boundaries, and higher-order superstructures influence the mechanical properties considerably. The different kinds of block structures and their effects on domain formation and phase separation have been reviewed by Bonart [1].

Transmission electron microscopy (TEM) investigations of the morphology of the segmented block copolymers are typically relatively recent. Foks *et al.* [2] demonstrated a spherulitic-like structure and hard segment lamellae in polyurethanes based on poly(ethylene adipate) (molecular weight $M_n = 2000$) and p,p'-diphenylmethyl diisocyanate (MDI) and 1-4-butanediol. According to Bonart [1] the statistical distribution of hard segment length would give rise to extended chain hard segment crystallinity and diffuse domain boundaries. However, Foks *et al.* [2] found very sharp boundaries and concluded that the hard segments were crystallized into lamellae of sizes not related to the length of the hard segments. In a later investigation [3] Foks *et al.* investigated the same system with replica-TEM techniques and found that hard segment contents between 32 and 50% showed two types of grain aggregates dispersed in spherulite-like matrix while 22% hard segments did not show any traces of crystallinity. Fibrils of hard segment crystallinity arranged in spherulitic structures were also observed by Fridman *et al.* [4, 5] in poly(propylene oxide) based polyurethanes.

Polyether-ester type multiblock copolymers were investigated by Cella [6]. Hard segment crystalline lamellae up to 10 nm in width, in some cases only about 3 nm, but several hundreds of nanometres in length were observed. The broad distribution of hard segment length in the copolymer chains resulted in incomplete crystallization. The shortest were presumably too short to crystallize and some of the longest were prevented from being incorporated into the crystalline lattice because of chain entanglements. The crystallinity was thought to be of folded chain type with many tie molecules interconnecting different crystalline domains and thus giving a crystalline phase continuity. The glass transition temperature of the soft phase was increased with increasing hard segment content. This was explained as at least partly due to the increased level of pseudo-crosslinking between the crystalline domains and the fact that many hard segments were still molecularly dispersed throughout the elastomeric phase.

* Author to whom all correspondence should be sent.

0022–2461/91 $03.00 + .12

Polyamide containing multiblock copolymers differs from the previous two types in that the segment length distribution is narrow for both blocks due to the anionic polymerization of the polyamide segments normally used. RIM materials based on polyamide 6, PA6, have been studied by Hedrick *et al.* [7, 8]. They described a RIM-procedure based on acyllactam initiated PA6 polymerization from the endgroups of the prepolymer, i.e., the acyllactam ended polyol. A multiblock constitution was suggested due to transfer reactions. This was verified by Kurz [9] using selective degradation of the final polymers and size exclusion chromatography (SEC) analysis of the species. Using polypropyleneglycol (PPG) as soft segments the melting point of the crystalline PA6 phase decreases linearly with increasing polyol content [7, 9] and the crystallinity is reduced at higher polyol contents [9]. Dynamic mechanical data show extensive phase separation with slightly lower soft segment peak temperatures for the polymers with the lowest polyol content (< 20%). In a recent paper [10] describing multiblock copolymers consisting of polyamide 12 and poly(tetra methylene glycol), PTMG, a less extensive phase separation is deduced from dynamic mechanical data. In this work the morphology of the multiblock copolymer was also investigated using TEM. In contrast to the polyurethanes and polyether-esters described earlier there were no signs of a spherulitic structure on any scale. Samples with block length ratios PA12/PTMG of 4/1, 2/2 and 2/1 all showed PA12 crystalline lamellae of widths 5–10 nm. The interlamellae phase was supposed to be mainly amorphous PTMG, contrasted with OsO_4 staining. The block sizes in polymers studied were comparatively small. The M_n of PA12 blocks were 2000 or 4000 and of the PTMG blocks only 1000 or 2000.

The morphology of the polyamide block copolymers is still not fully understood. The molecular weight of the blocks must be critical in this low molecular weight range, where entropy contributions start to promote some miscibility. The sharpness of the phase boundaries and the shape of the phases depend on the strength of the driving force for phase separation. The polymer chains must be able to maintain not too strained conformations and the phases must be given their appropriate density. These effects restrict the driving force of phase separation. However, the driving force for crystallization is very strong and even the strongest specific interaction cannot prohibit crystallization. It can only affect the crystallization kinetics [11]. This work is aimed at clarifying the morphology of some typical polyamide block copolymers of RIM-type. As soft segment polyol polybutadiene has been chosen to allow indisputable selective staining from OsO_4 for use in TEM.

2. Experimental details

2.1. Materials

Three formulations of polyamide 6 (PA6) RIM material were polymerized and supplied by Monsanto. They were designated P3A 2000, P3A 3000 and P3A 4000 and contained 20, 30 and 40% by weight of prepolymer, respectively. The prepolymer was a polybutaniene (PB) of molecular weight around 2000 with acyllactam endgroups. The specimens were delivered in 4 mm thick sheets. The details concerning the polymerization has been given elsewhere [7, 8]. According to the polymerization conditions the molecular weight of the PA6 blocks should be of the order of 3000 to 1200 depending on PB content [9].

A pure PA6 in granular form supplied by Aldrich was used for comparison in the calorimetric and dynamic mechanical tests.

2.2. Thermal analysis

A Mettler TA 2000 DTA apparatus was used to determine the T_m and crystallinity of the polyamide phase. The tests were run at 10 °C min^{-1} on samples of 6–7 mg weight.

2.3. Dynamic mechanical tests

Complex tensile modulus and damping factor tan δ measurements were performed on a Rheovibron DDV II C working at 11 Hz in tensile mode. The 0.1–0.2 mm thick specimens were compression moulded from the thick sheets and slowly cooled. They were dried in a vacuum oven at 85 °C for 23 h prior to testing.

2.4. Wide angle X-ray scattering (WAXS)

WAXS studies were carried out with samples of thickness 1 mm. The intensity was recorded as a function of scattering angle (2θ) using a Philips PV1700 diffractometer.

2.5. Transmission electron microscopy (TEM)

A JEOL 2000 EX STEM/TEM was used. Some care must be taken to avoid artefacts due to beam damage of the specimens, especially destruction of the crystallinity. The magnification of the microscope was calibrated and the beam current carefully measured. A condenser lens aperture 2 and spot size 3 resulted in a beam current of 2.2 nA. An exposure time of four seconds at 10 000 times magnification results in an exposure of 112 C m^{-2}. This is sufficient to destroy the diffraction pattern in polyethylene. However, PA6 is found to resist twice [12] or six times [13] that dose. Thus 10 000 times magnification and 200 kV acceleration voltage was used for the studies. Thin specimens were cut at room temperature with a diamond knife equipped microtome, LKB Ultratome V. The approximately 100 nm thick samples were stained in OsO_4 vapour from 30 minutes to 24 h. The samples were examined without prior carbon deposition.

3. Results

3.1. Electron microscopy

The TEM micrographs show different kinds of morphology depending on butadiene content. 20% PB, Fig. 1, gives a continuous network of PA 6 lamellae

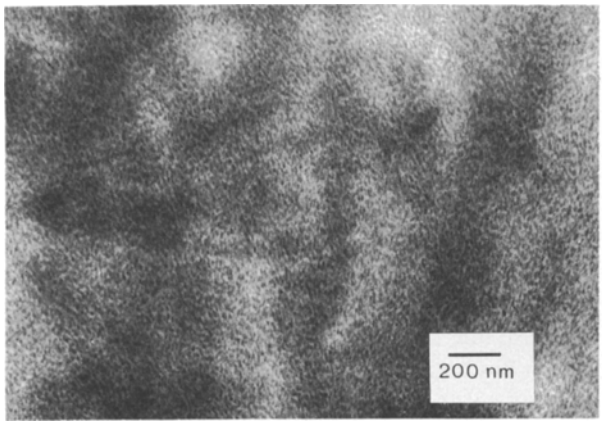

Figure 1 Transmission electron micrograph of PA6/PB block copolymer with 20% PB by weight.

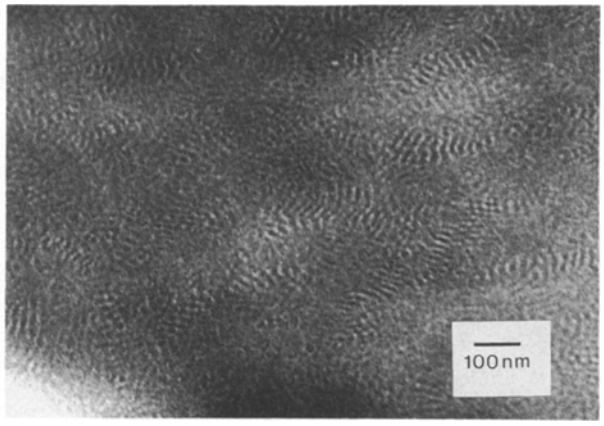

Figure 3 Transmission electron micrograph of PA6/PB block copolymer with 40% PB by weight.

surrounding spherical or slightly elongated droplets of PB. The PB-phase is dark due to the contrast from OsO_4 staining. The presence of phase contrast in this micrograph may lead to misinterpretation [14] but with support from the following micrographs with more lamella like morphologies, and with the defocusing problem taking into account, we estimate the dimensions of the dark PB phase domains to be around 10 nm and the PA6 lamellar width to be around 15 nm. A root-mean-square end to end distance for a PB chain with molecular weight 2000 is 6.7 nm using a 0.5 nm repeat unit length and 4.75 as the correction factor for steric hindrance. Since the chain is a block in a block-copolymer the conformational possibilities are restricted and 6.7 nm can be regarded as a minimum value.

Fig. 2 shows the morphology of the block copolymer containing 30% PB. The PB phase is more lamella-like and the PA6 lamellae are thinner. A dual phase continuity is now nearly developed but is fully developed when the PB-content increases to 40%, Fig. 3. The dimensions of the phases are now approximately 10–15 nm.

A higher magnification on the blockcopolymer containing 40% PB, Fig. 4, reveals a substructure. The dark domains are subdivided by very thin light bands oriented perpendicular to the large domain direction.

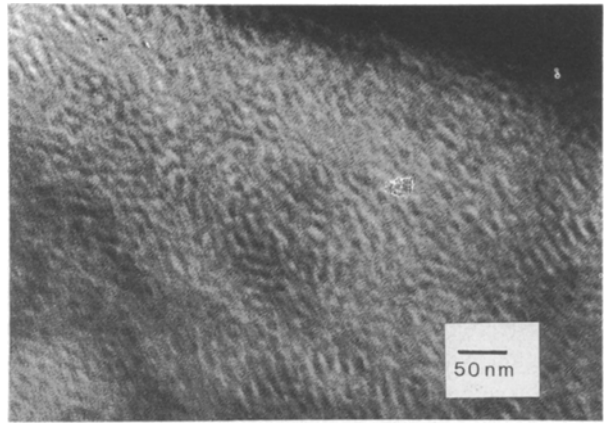

Figure 4 Same as Fig. 3 but higher magnification.

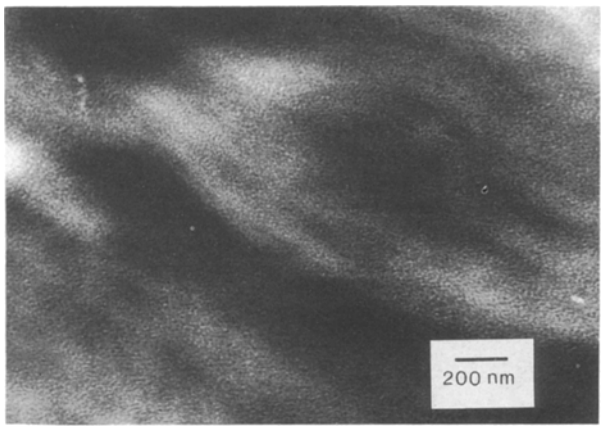

Figure 2 Transmission electron micrograph of PA6/PB block copolymer with 30% PB by weight.

Corresponding very thin dark bands are also found in the light domains. This substructure has also been found, though less clearly, and after very close examination of the negatives, in the block-copolymers with 20 and 30% PB. The substructure can only be seen in very thin parts of the specimens, which has been achieved in Fig. 4. In order to avoid artefacts from the conductive layer of the specimen, the micrographs in Figs 3 and 4 have been taken without a carbon deposition layer.

Fig. 4 suggests that two levels of morphology exist. The domains seen in Figs 1–3 should thus contain both kinds of blocks, but of course in very different proportions.

3.2. Dynamic mechanical properties

Small strain complex elastic modulus and loss factor tan δ were determined over a broad temperature range at 1 °C min^{-1} heating rate. Fig. 5 shows the complex modulus against temperature for the different block copolymers and for PA6. The drop in modulus around − 80 °C is attributed to the glass transition of the PB-phase and the drop at 60 °C to 80 °C to the glass transition temperature of the PA6. The effects of the PA6 crystalline melting start at 200 °C. The character of the curves agrees with the dynamic mechanical data reported for PA6-polypropylene glycol (PPG) block

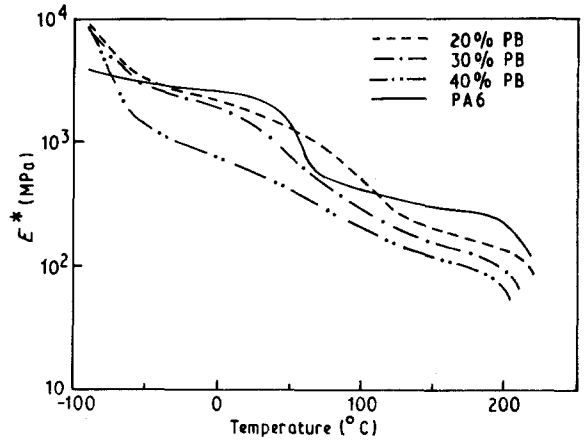

Figure 5 Complex tensile modulus for the block copolymers and PA6 against temperature.

copolymer [9]. The modulus decrease between the two glass transition temperatures is much larger for the block copolymers compared to PA6. In a block copolymer with longer blocks and perfect phase separation the difference should be negligible. The larger slope shown here and the composition dependent location of the modulus drop associated with the PA6 glass transition is either a result of incomplete phase separation or an effect of very short blocks. The tan δ peaks from the materials shown in Fig. 6 further demonstrate the phase separation situation. The peak associated with the PA6 glass transition is substantially broadened and shifted upwards in temperature. The same situation was observed by Kurz [9] for PA6-PPG block copolymers and was explained to be due to small differences in moisture content. We cannot fully exclude the possibility of moisture uptake during the testing though the specimens were carefully dried before test. However, it is interesting to note, that the level of the mechanical loss around the PA6 glass transition is independent of soft segment content. This is also in accordance with Kurz [9] data showing this high level of damping even at soft segment contents of 65%.

The low temperature peaks associated with the PB glass transition are composition dependent and show a sharpness characteristic of a pure amorphous polymer. This suggests an almost complete phase separation inspite of the low molecular weights of the blocks. The peak temperature increases slightly with soft segment contents. This was also found by Kurz [9] for the PA6-PPG block copolymers, but less extensive. If the peak shifts were due to partial miscibility they should have the opposite signs, i.e. the peak from the highest PB containing polymer would have the lowest peak temperature. In our case the peak shifts are due to some conformational restrictions on the PB blocks associated with the differences in morphology according to the micrographs Figs 1–4. We conclude from the dynamic mechanical tests that our block copolymers are completely phase separated, as was the case for PA6-PPG block copolymers [7–9]. Block copolymers of PA12-PTMG [10] were much less phase separated.

3.3. Thermal and X-ray analysis

The crystalline phase of the PA6 plays a major role in the phase separation process resulting in the observed morphology. A closer examination of the PA6 crystallinity in the block copolymers and comparison with neat PA6 is thus necessary. The melting temperatures and the enthalpies of melting of the PA6 contents for the block copolymers and neat PA6 are shown in Fig. 7. The decrease in PA6 crystalline melting point with increasing PB content is quantitatively in agreement with data reported for PA6-PPG block copolymers [7, 9], with the exception of pure PA6 where they reported only 215 °C. However, the melting point of high molecular weight PA6 is strongly dependent on thermal prehistory.

The melting enthalpy data show qualitative agreement with the data from Kurz who reported higher values throughout. However, up to 40% soft segment content results in higher melting enthalpies than are found in pure PA6. The more flexible environment in

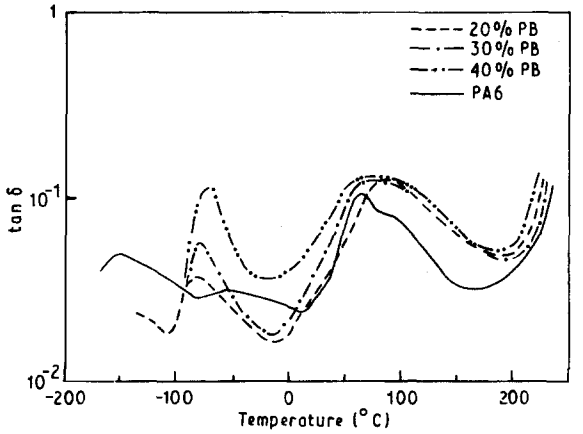

Figure 6 tan δ against temperature for the block copolymers and PA6.

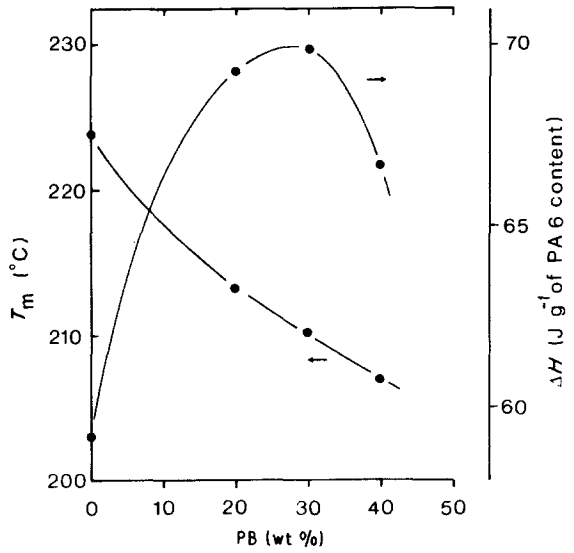

Figure 7 Melting temperature and melting enthalpy for the block copolymers against PB content.

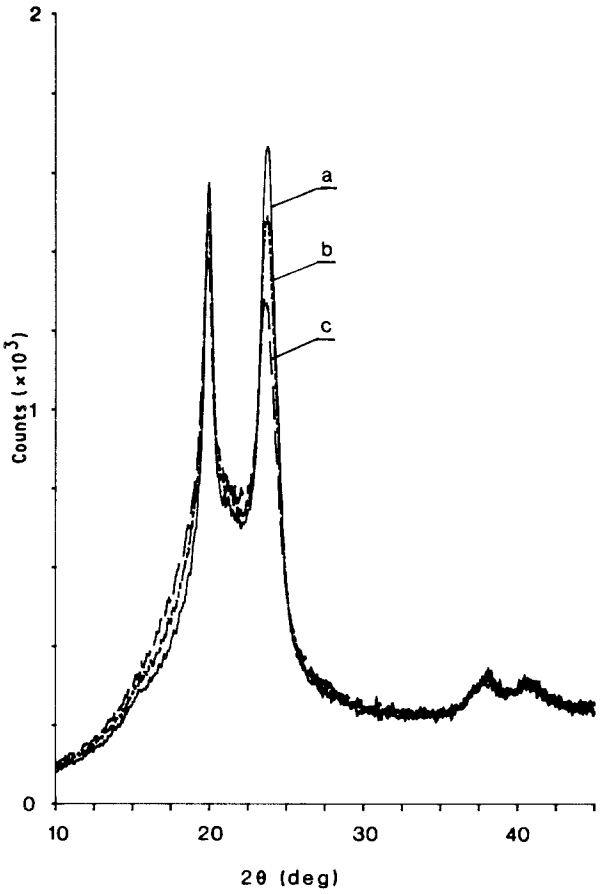

Figure 8 WAXS scans of the block copolymers. a, b and c represent 20, 30 and 40% PB, respectively.

the block copolymers obviously enhances the possibility of crystallization.

The WAXS data from the block copolymer, Fig. 8, show very sharp peaks indicating high crystalline perfection. The location of the two peaks identifies the α-form crystals [15] and suggests a folded chain morphology. The two peaks at about 20 degrees and 23.9 degrees double diffraction angle are identified as the (2 0 0) and (0 2 0) reflections, respectively [15].

4. Discussion

The constitution of the block copolymers is determined by the RIM process which has been analysed in detail [7–9]. The hydroxyl ended soft segment, i.e. the polyol, reacts with bis-acyllactam to form the prepolymer, which in the final RIM processing step initiates and takes part in the caprolactam polymerization. At first sight it seems most likely that a triblock copolymer should be formed, but the ester and amide linkages in the prepolymer can work as initiation and transfer sites, thus forming a multiblock copolymer. Kurz has shown that the latter is true using SEC analysis of the products as well as the PA6 species formed by oxidative degradation separating the blocks. As long as the polyol itself does not contain molecular groups that can act as transfer sites the polymerization must be the same as for the RIM system investigated by Kurz [9]. We therefore conclude that our copolymers based on polybutadiene polyol have the same constitution. Thus the PA6 blocks in our copolymers with 20, 30 and 40% by weight PB most likely have PA6 blocks with molecular weights 3000, 2000 and 1900, respectively, according to Kurz SEC measurements. The number of blocks increases with increasing soft segment content and every chain is terminated with PA6 blocks.

Though the blocks are very short the micrographs and the dynamic mechanical data show a very complete phase separation and the calorimetric data show an extent of crystallization even higher than in pure PA6. The decrease in melting temperature is hardly due to diluent effects since the phase separation is almost complete. Consideration of the very short blocks leads to the suggestion that the melting point should be related to the molecular weight through the modified Flory equation

$$(1/T_m) - (1/T_m^0) = 2R/(\Delta H^0 X_n) \quad (1)$$

where T_m^0 is the equilibrium melting point, R the gas constant, ΔH^0 the heat of fusion of the crystal in equilibrium and X_n the degree of polymerization.

Kurz [9] has found good agreement between molecular weights determined from the above relation and his SEC results. However, choosing the appropriate values for T_m^0 and ΔH^0 for PA6 is not unambiguous. Critical discussions on that subject by Wunderlich [16] lead to an equilibrium melting point, T_m^0, of 270 °C and ΔH^0 to 230 J g^{-1} as the best suggestions. With those values inserted in the above relation, the molecular weights are unreasonably low. The reason for this is that the modified Flory equation rather expresses the dependence of the equilibrium melting point on the degree of polymerization, and the measured melting point from the DCS on melt crystallized material is far from representing equilibrium conditions.

According to the micrographs, the phase boundaries are quite sharp, at least for 40% PB content, suggesting extensive chain folding. The folding period naturally affects the melting point irrespective of chain length. In our case with very short blocks and restrictions from the separated PB-phase very short folding periods are likely even in very annealed material. The decrease in melting point should therefore be due to decreased lamellar thickness in the copolymers, as expressed in the Thomson-Gibbs equation [17]

$$T_m = T_m^0(1 - 2\gamma/(l\Delta h_f')) \quad (2)$$

where γ is the specific surface free energy, l the lamellar thickness and $\Delta h_f'$ the bulk heat of fusion per volume. T_m^0 is chosen to be 543 K, $\Delta H^0 = 230$ J g^{-1}, $\rho_c = 1235$ kg m^{-3} and $\gamma = 80$ mJ m^{-2} [17]. For the three copolymers with 20, 30 and 40% PB this gives lamellar thicknesses of 5.7, 5.1 and 4.9 nm, respectively. Lamellar thickness of 5–6 nm are reported from solvent cast α-form crystals [17]. About 6 nm has been determined as the shortest fold length in quenched specimens [18] of unannealed melt crystallized α-form with small angle X-ray diffraction (SAXD). Our WAXS data can give some information on the same subject through the Scherrer equation

$$L_{hkl} = K\lambda/(\beta_0 \cos\theta) \quad (3)$$

where L_{hkl} is the crystal size normal to the specified plane, K is a constant near unity, λ the wavelength of the X-ray radiation (in our case 0.1540 nm from CuK_α radiation), β_0 the breadth in radians at the half-maximum intensity of the pure reflection profile and θ the diffraction angle. For the (0 2 0) peak in Fig. 8 we get for the copolymers containing 20, 30 and 40% PB, 4.5, 3.3 and 2.9 nm crystal size, respectively. It is interesting to note that the dimensions calculated from the Thomson-Gibbs and Cherrer equations agree fairly well with domain sizes found in the micrographs, bearing in mind that the crystallinity is about 20–35% depending on the choice of ΔH^0.

In conclusion, the PA6/PB block copolymers have been found to form morphologies consisting of well separated phases. The PA6 blocks easily form a semi-crystalline phase. The dimensions of the lamellar-like features in the micrographs show fair agreement with dimensions expected from melting point depression and WAXD data. The lamellar arrangement resembles what has been found for segmented polyether-esters [6] in contrast to the results from analysis on segmented polyurethanes [2–5] showing spherulitic morphologies. In the case of PA12/PTMG block copolymers [10] the lamellar arrangement again shows similarities with what we found for PA6/PB with high PB content, but the micrographs of PA12/PTMG showed sharper boundaries between stained and unstained areas. This can be explained by the fact that PA12/PTMG showed partial miscibility and thus the amorphous parts of the PA12 are included in the stained phase. The segmental arrangements in the PA6/PB block copolymers are most probably of the same type as has been proposed for the segmented polyether-esters [6]. We suggest that the PA6 phase consists of folded chain lamellae surrounded by amorphous PA6. With high PA6 content partly parallel lamellae may exist surrounded by more amorphous PA6 thus forming domains that are thicker in relation to their length. The thickness of the PA6 lamellae is determined by the crystallization conditions but substantially thicker lamellae are most probably prohibited by the short block length. Longer folding periods make the rejection of the PB blocks from the PA6 phase more difficult if the level of crystallinity is maintained. At 40% PB content the two phases occupy almost the same volume, leading to the lamellar-like morphology seen in Fig. 3. Individual chains are distributed over different lamellae, thus forming an interconnected structure. Since the dynamic mechanical results show extensive phase separation and the OsO_4 staining is very specific for the PB, we conclude that stained areas consist of PB only. With this in mind the fine structure shown in Fig. 4 is very interesting.

The PA6 lamellae seems to have been interrupted by very thin layers of PB. Corresponding thin layers of PA6, presumably amorphous, are visible in the PB domains. The fine structure may be the result of a compromise between phase separation and crystallization on the one hand and restrictions due to short block length on the other. However, for the moment we cannot fully rule out the fine structure's being an artefact. Conclusions on the morphology presented here are most probably also applicable to the more frequently used PA6/PPG RIM materials. The chemistry of the polymerization is quite the same. The phase separation according to dynamic mechanical results and the crystallization behaviour [9] show great similarities.

Acknowledgement

The National Swedish Board for Technical Development STU is acknowledged for financial support.

References

1. R. BONART, *Polymer* **20** (1979) 1389.
2. J. FOKS, G. MICHLER and I. NAUMAN, *ibid.* **28** (1987) 2195.
3. J. FOKS and H. JANIK, *Pol. Eng. Sci.* **29** (1989) 113.
4. I. D. FRIDMAN and E. L. THOMAS, *Polymer* **21** (1980) 388.
5. I. D. FRIDMAN, E. L. THOMAS, L. J. LEE and Ch. M. MACOSKO, *Polymer* **21** (1980) 388.
6. R. J. CELLA, *J. Polym. Sci., Polym. Symp.* **42** (1973) 727.
7. R. M. HEDRICK and J. D. GABBERT, 91st National AIChE Meeting, Detroit MI, 17 August, 1981.
8. R. M. HEDRICK, J. D. GABBERT and M. H. WOHL, in "Reaction Injection Moulding", edited by J. E. Kresta (ACS Symposium Series 270, 1985) p. 135.
9. J. E. KURZ, *Polymer Process Engineering* **3** (1985) 7.
10. H. BOUBLIL, E. OKOROAFOR, M. BELHOUCINE and J. RAULT, *Polym. Eng. Sci.* **29** (1989) 679.
11. D. R. PAUL and J. W. BARLOW, "Polymer Alloys II, Polymer Science and Technology", Vol. 11, edited by D. Klempner and K. C. Frisch (Plenum Press, New York, 1980) pp. 239–53.
12. K. KOBAYASHI and K. SAKAOKU, *Laboratory Investigation* **11** (1965) 359.
13. M. S. ISAACSON, "Specimen Damage in the Electron Microscope from Principles and Techniques of E. E. M. Biological Applications", Vol. 7, edited by M. Hayat (Van Nostrand-Reinhold, New York, 1977) p. 1.
14. E. J. ROCHE and E. L. THOMAS, *Polymer* **22** (1981) 333.
15. P. H. GEIL, "Polymer Single Crystals, Polymer Reviews", Vol. 5 (Wiley & Sons, New York, 1963) p. 37.
16. B. WUNDERLICH, "Macromolecular Physics", Vol. 1 (Academic Press, New York, 1973).
17. *Idem., ibid.*, Vol. 3 (1980).
18. M. HIRAMI, *Macromol. Chem.* **183** (1982) 2857.

Received 13 March
and accepted 3 December 1990